

# LEARNING FROM HETEROGENEOUS EEG SIGNALS WITH DIFFERENTIABLE CHANNEL REORDERING

Aaqib Saeed<sup>1\*</sup>, David Grangier<sup>2</sup>, Olivier Pietquin<sup>2</sup>, Neil Zeghidour<sup>2</sup>

<sup>1</sup>Eindhoven University of Technology, Eindhoven, The Netherlands

<sup>2</sup>Google Research, Paris, France

## ABSTRACT

We propose *CHARM*, a method for training a single neural network across inconsistent input channels. Our work is motivated by Electroencephalography (EEG), where data collection protocols from different headsets result in varying channel ordering and number, which limits the feasibility of transferring trained systems across datasets. Our approach builds upon attention mechanisms to estimate a latent reordering matrix from each input signal and map input channels to a canonical order. *CHARM* is differentiable and can be composed further with architectures expecting a consistent channel ordering to build end-to-end trainable classifiers. We perform experiments on four EEG classification datasets and demonstrate the efficacy of *CHARM* via simulated shuffling and masking of input channels. Moreover, our method improves the transfer of pre-trained representations between datasets collected with different protocols.

**Index Terms**— eeg, electroencephalogram, convolutional network, self-attention, seizure, transfer learning

## 1. INTRODUCTION

Electroencephalography (EEG) is the measurement of the brain’s electrical activity, which informs about neural functions and related physiological manifestations [1]. It is generally collected along the scalp in a non-invasive way for a wide array of tasks, including for clinical purposes and Brain-Computer Interface (BCI) systems. Automatic classification of EEG signals with machine learning has been widely adopted to study, diagnose, and treat neurological disorders such as seizures, epilepsy, Alzheimer’s, and sleep-related problems [2, 3, 4]. In BCI tasks, EEG is used to capture motor imagery signals and recognize user’s intents [5] and event-related potential [6]. Likewise, it is also used to estimate mental workload or task complexity for monitoring cognitive stress and performance [7].

Over the last years, automatic EEG classification has moved from using hand-crafted features [8, 9] towards learning high-level representations from raw EEG signals with deep neural networks [10, 11]. In particular, Convolutional Neural Networks (CNNs) have become the standard architecture to process EEG signals and have been used for many tasks including motor imagery [12, 13, 14], seizure prediction [15, 16], Parkinson diagnosis [17] and sleep stage scoring [4]. Nevertheless, EEG measurements remain notoriously subject to intra- and inter-subject variability, which makes generalization particularly challenging and led to numerous works focusing on the reduction of this generalization gap [18, 19, 20]. A less explored problem is the variability due to measuring devices: different EEG headsets have a varying number of

electrodes (from a few to dozens) and different electrical specifications [21]. Moreover, it is not rare that headset malfunctions lead to noisy or even missing channels. Consequently, available EEG datasets are heterogeneous, and the majority of them are very small.

Scaling EEG training data seems, therefore, only feasible by aggregating heterogeneous datasets. This requires devising novel classification methods that are robust to permuted and missing channels since classical CNNs assume a fixed number of input channels, ordered consistently across data examples. With this objective, we introduce a new framework for training a single CNN across varying EEG collections that can differ both in number and location of electrodes. Our CHANNEL Reordering Module (CHARM) ingests multichannel EEG signals, identifies the location of each channel from their content, and remaps them to a canonical ordered set. After this remapping, the channels are ordered consistently and can be further processed by a standard neural network, regardless of the actual variations in the input data. We evaluate CHARM on three tasks: seizure classification, detection of abnormal EEGs and detection of artifacts (e.g. eye movement). We show that CHARM is significantly more robust to missing and permuted channels than a standard CNN. We also introduce a data augmentation technique that further improves the robustness of the model. Moreover, we show for the first time that pre-training representations of EEG on a large dataset transfers to another, smaller dataset collected with a different headset.

## 2. METHODOLOGY

Our proposal is a differentiable reordering module that maps inputs with inconsistent channels to a fixed canonical order. It can be composed with further modules expecting consistent channel placement to be trained end-to-end on data without channel ordering information. As inputs, we consider EEG signals with an unknown channel ordering and potentially missing channels, (Figure 1). Our module takes these channels and reorders them to a canonical, consistent order prior to further processing. Precisely, our reordering module outputs a soft reordering matrix  $p$ .

The input signal  $\mathbf{x} \in \mathbb{R}^{N \times T}$  is a recording over  $N$  channels for a duration  $T$ . Considering  $M$  canonical channels, the reordering matrix  $p(\mathbf{x})$  is an  $N \times M$  matrix. Precisely, each canonical output is estimated as a weighted sum of the input channels, i.e.,

$$\hat{\mathbf{x}}_{i,t} = \sum_{j=1}^N p(\mathbf{x})_{i,j} \mathbf{x}_{j,t}, \quad i = 1, \dots, M, \quad t = 1, \dots, T. \quad (1)$$

$\hat{\mathbf{x}} \in \mathbb{R}^{M \times T}$  then serves as input to a standard neural network expecting a consistent input ordering across data samples. Since  $p$  is differentiable, the reordering module parameters can be learned

\*This work was conducted while interning at Google.

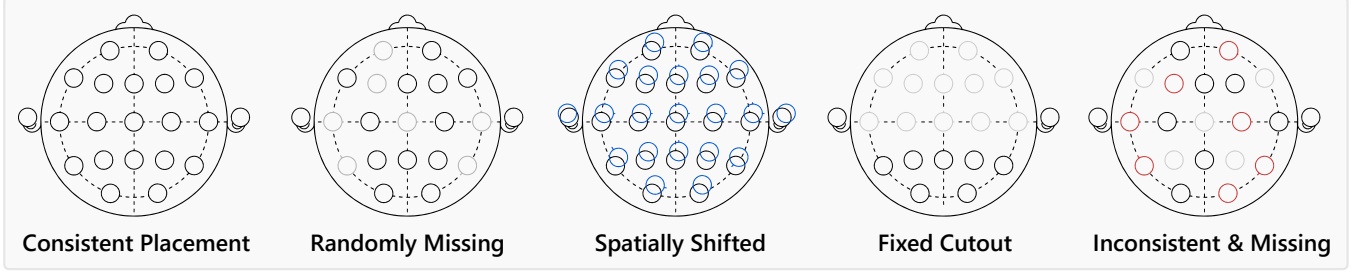


Fig. 1. Illustration of various forms of inconsistencies that can arise in EEG recordings.

jointly with the rest of the architecture (Figure 2). Training optimizes the cross-entropy classification loss with no extra supervision on the channel order.

## 2.1. Learnable Channel Remapping

Using *CHARM* as the first layers of the model allows us to train a single deep architecture over different EEG recording headsets. We consider three variants of our reordering method.

### 2.1.1. Convolutional Reordering

*CHARM-base* represents the signal of each channel as a vector,

$$h_i = m^{\text{conv}}(\mathbf{x}_{i,:}) \quad (2)$$

where  $m^{\text{conv}}$  composes a 1-D convolution layer with  $d$  filters and an aggregation operation (global max-pooling) to map a single-channel temporal signal into a fixed dimensional vector of dimension  $d$ . Since this step convolves channels independently, its predictions are invariant to a reordering of the input channels.

Each vector is then compared to learned embeddings of dimension  $d$  that represent each of the  $M$  canonical channels,  $c \in \mathbb{R}^{M \times d}$ , yielding the matrix  $p$  for channel remapping,

$$p_{i,j} = \text{softreorder}(c, h)_{i,j} = \frac{\exp(c_i \cdot h_j)}{\sum_{j'} \exp(c_i \cdot h_{j'})}. \quad (3)$$

### 2.1.2. Attentive Reordering with Canonical Keys and Values

*CHARM-CKV* builds upon residual attention [22]. We build a *query vector* representing each input channel as  $q_i = m^{\text{conv}}(\mathbf{x}_{i,:})$ . Each query vector *attends* over canonical channels, i.e. each input channel query is mapped to a weighted sum of canonical channel *value vectors* according to their similarity to canonical *key vectors*,

$$h_i = \sum_j a_{i,j} v_j \quad \text{where} \quad a_{i,j} = \frac{\exp(q_i \cdot k_j)}{\sum_{j'} \exp(q_i \cdot k_{j'})}, \quad (4)$$

and  $k, v$  are key and value embeddings representing the canonical channels. These layers can be stacked after a residual connection,

$$q_i^{l+1} = \text{layernorm}(q_i^l + \text{mlp}^l(h_i^l)) \quad (5)$$

where  $q^l, h^l$  are the query and attentive representations of layer  $l$ . `layernorm` denotes a layer normalization module [23] and `mlp` denotes a multi-layer perceptron with a single hidden layer. We denote the residual attention compactly as

$$q_i^{l+1} = \text{attn}(q_i^l, k, v) \quad (6)$$

At the last layer, we compute  $p = \text{softreorder}(c, q^l)$ .

Compared to our base convolutional model, this model can use many channel predictions to refine each individual prediction. For instance, it can be confident only for a few channels at the first layer and refine its decision for the other channels in the next layers.

### 2.1.3. Attentive Reordering with Canonical Queries

*CHARM-CQ* reverses the role of canonical and input channels, using input keys and values and relying on canonical queries. Input keys and values result from an independent channel-wise convolution with 1D filters,

$$(k_i, v_i) = m^{\text{conv}}(\mathbf{x}_{i,:}) \quad (7)$$

and initial canonical queries  $q$  are learned embeddings. Each query can be attended over to represent each *canonical channel* as a weighted sum of *input* values, as in Equation 6. Several layers of attention can be stacked. Finally,  $p = \text{softreorder}(q^l, k^l)$ .

In our experiment, we found it beneficial to share keys and values across layers, i.e.  $(k^l, v^l) = (k^0, v^0)$ .

## 2.2. CMSAugment: shuffling and masking channels

Data augmentation is another strategy to improve the generalization to inconsistent inputs. As an orthogonal contribution to our remapping module, we propose a CHANNEL MASKING AND SHUFFLING AUGMENTATION (CMSAugment) strategy. During training, CMSAugment first shuffles the channels and next samples a binary mask over channels to drop some channels entirely, with a uniform distribution from 0 masked channels to  $N - 1$ . In Section 3, we show how it significantly helps a simple CNN becoming robust to missing and inconsistent channel placements, with the best results being obtained by combining *CHARM* and CMSAugment.

## 2.3. Network Architecture Design and Implementation

Our main architecture is a 1D-CNN that takes raw EEG signals as input and cascades four blocks of 1D convolutions. Each block has a LayerNormalization [23] and PReLU [24] as activation along with a max-pooling layer for downsampling. We use a kernel size of 8 with stride 1 and pooling size of 2 and stride 2 with 256 feature maps for the first three blocks, and 512 in the last one. To aggregate the features, we use global max-pooling, which then feeds into a single linear classification layer. We apply L2 regularization with a rate of  $10^{-4}$  on all the layers but the last. Given an input sequence, we first apply an InstanceNormalization [25], which normalizes each channel independently. Then our baseline model (Baseline) passes the output through the 1D-CNN directly. On the other hand, *CHARM*

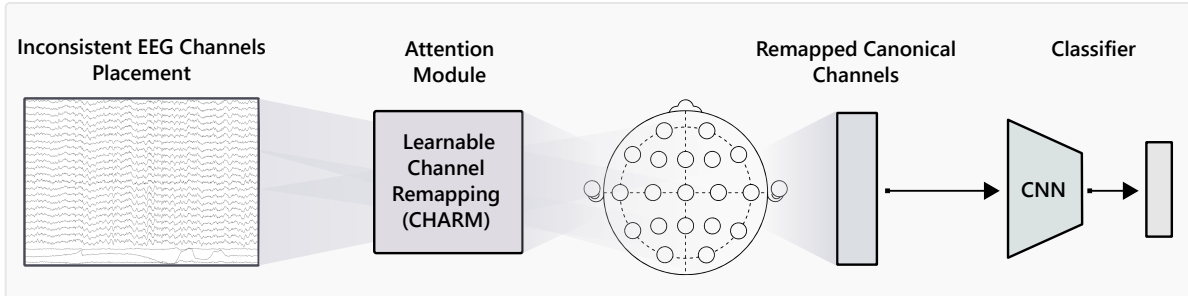


Fig. 2. Overview of CHARM with a 1D convolutional classifier for EEG classification tasks.

first passes the waveforms through the remapping module, which then feeds into the 1D-CNN.

### 2.3.1. Channel Remapping Networks

*CHARM* uses 24 canonical channels, regardless of the actual number of channels in an input sequence (from 17 to 22 in our experiments). We represent each canonical channel with an embedding of dimension  $d = 32$ . *CHARM-base* contains three convolutional layers with 32 feature maps and a filter size of 8 with a stride of 1. The residual attentive modules are inspired by Transformers [22]. Queries, keys and values have a dimension of 32, and the mlp has a single hidden layer of dimension 64. For all models, we apply  $L1$  regularization onto  $p$  with a weight of  $10^{-4}$  to promote sparse reordering matrices.

### 2.3.2. Training Details

We train on 500-sample windows dynamically sampled from an entire EEG sequence. *CHARM* is trained jointly with the 1D-CNN to minimize a categorical cross-entropy loss, using ADAM [26] with a learning rate of  $10^{-4}$  and a batch size of 64 for 100 epochs. For imbalanced datasets (Section 3), we use a weighted cross-entropy loss to minimize error across rare and frequent classes equally.

## 3. EXPERIMENTS

Our evaluation focuses on the Temple University Hospital EEG Corpus (TUH) [27] and CHB-MIT dataset [28]. The TUH corpus is the most extensive publicly available corpus with over 15000 subjects; it comprises several datasets analyzed and annotated by expert clinicians where the majority of EEG is sampled at 250Hz [27]. The CHB-MIT contains intractable seizures collected from 23 pediatric subjects at a sampling rate of 256Hz. Here, we focus on the tasks of recognizing abnormal EEG (TUH Abnormal), detection of artifacts such as eye movement or chewing (TUH artifacts) as well as determining the presence and type of seizures (TUH Seizure, CHB-MIT). Each dataset has a different number of EEG channels, as shown in Table 1. We employ a 10-folds stratified cross-validation technique for assessing the model performance. Our evaluation metric is the accuracy averaged over ten folds, weighted for imbalanced datasets (TUH Artifacts, TUH Seizure) to account for minority classes.

### 3.1. Generalizing to shuffled and masked channels

Table 1 compares *CHARM* to a baseline 1D-CNN when generalizing to noisy conditions. The models are trained on *clean* (no masking, no shuffling) channels, but the evaluation is done under different forms

of noise injection. To this end, the *Noisy* entries in Table 1 indicate performance when the test input channels are shuffled and 0 to  $N - 1$  channels are uniformly masked. Similarly, *Noisy- $n\%$*  represents the results when a fixed ratio of  $n\%$  channels are masked at random after shuffling. We first observe that when evaluating on clean inputs, the baseline model performs better. This can be explained by the fact that *CHARM* sees channels independently and cannot exploit ground-truth channel location, which is useful when training and evaluating on identical channels. On the other hand, *CHARM*-based remapping techniques perform significantly better in handling permuted and masked channels across all four datasets. Even when 50% to 75% channels are missing, our proposed approach maintains high accuracy. In particular, on TUH Seizure/*Noisy-75%* *CHARM-CQ* attains 0.704 accuracy, against 0.171 for the baseline.

### 3.2. Performance in structured masking conditions

Table 2 reports the performance on TUH Seizure when only a subset of the channels from a specific half of the brain is active, a more tangible setting than random masking. We split the electrodes along a vertical or horizontal axis and evaluate on each half separately (Group<sub>A</sub> and Group<sub>B</sub>). We train the models either on clean inputs or with CMSAugment, and do not report results for *CHARM-base* since it performed worse than alternatives in previous experiments. When training without augmentation, *CHARM* significantly outperforms the baseline in most cases, reaching its best results when combined with CMSAugment. Interestingly, the robustness of the baseline system significantly improves when trained with CMSAugment. This shows that, independently of *CHARM*, data augmentation is also a promising avenue for robust EEG classification.

### 3.3. Transfer learning

So far, we assessed the performance individually for each task, simulating different headsets with random shuffling and masking. Now, we evaluate the proposed methods in handling inconsistent channels in a real cross-dataset transfer learning setting. In [21], authors propose an algorithm to handle transfer between headsets, for a same subject, and using the common subset of channels shared between headsets. In contrast, *CHARM* does not require any knowledge about channel placement and exploits all channels of each headset. Moreover, we experiment in a more challenging setting: we transfer trained representations to a new headset, on new subjects. We pre-train the models with clean inputs on the TUH Seizure dataset in a standard way and discard the classification head. We then reuse the other layers for learning either a linear classifier on-top of a fixed network or fine-tune it entirely on the CHB-MIT dataset. Importantly, as the number of channels in CHB-MIT is lower than TUH

**Table 1.** Test accuracy ( $\pm$  std) averaged over 10-folds for model generalization to shuffled and masked input channels. The entries with Noisy- $n\%$  represent the results when a fixed ratio of  $n\%$  of the channels are masked after shuffling.

Dataset	Channels	Classes	Method	Clean	Noisy	Noisy-25%	Noisy-50%	Noisy-75%
TUH Abnormal	22	2	Baseline	<b>0.830 <math>\pm</math> 0.030</b>	0.566 $\pm$ 0.025	0.581 $\pm$ 0.025	0.589 $\pm$ 0.027	0.548 $\pm$ 0.028
			<i>CHARM-base</i>	0.766 $\pm$ 0.016	0.742 $\pm$ 0.014	0.760 $\pm$ 0.015	0.743 $\pm$ 0.016	0.731 $\pm$ 0.014
			<i>CHARM-CKV</i>	0.772 $\pm$ 0.019	<b>0.751 <math>\pm</math> 0.011</b>	<b>0.767 <math>\pm</math> 0.013</b>	<b>0.756 <math>\pm</math> 0.013</b>	<b>0.747 <math>\pm</math> 0.015</b>
			<i>CHARM-CQ</i>	0.751 $\pm$ 0.014	0.743 $\pm$ 0.022	0.744 $\pm$ 0.026	0.744 $\pm$ 0.024	0.741 $\pm$ 0.028
TUH Artifact	19	6	Baseline	<b>0.711 <math>\pm</math> 0.009</b>	0.243 $\pm$ 0.016	0.245 $\pm$ 0.026	0.176 $\pm$ 0.018	0.263 $\pm$ 0.022
			<i>CHARM-base</i>	0.618 $\pm$ 0.011	0.514 $\pm$ 0.028	<b>0.566 <math>\pm</math> 0.029</b>	0.517 $\pm$ 0.028	0.466 $\pm$ 0.028
			<i>CHARM-CKV</i>	0.628 $\pm$ 0.016	0.481 $\pm$ 0.028	0.521 $\pm$ 0.034	0.491 $\pm$ 0.026	0.452 $\pm$ 0.019
			<i>CHARM-CQ</i>	0.607 $\pm$ 0.009	<b>0.524 <math>\pm</math> 0.044</b>	0.538 $\pm$ 0.043	<b>0.531 <math>\pm</math> 0.046</b>	<b>0.505 <math>\pm</math> 0.043</b>
TUH Seizure	21	5	Baseline	<b>0.950 <math>\pm</math> 0.010</b>	0.289 $\pm$ 0.040	0.368 $\pm$ 0.037	0.297 $\pm$ 0.052	0.171 $\pm$ 0.046
			<i>CHARM-base</i>	0.906 $\pm$ 0.021	0.663 $\pm$ 0.015	0.818 $\pm$ 0.026	0.693 $\pm$ 0.034	0.502 $\pm$ 0.027
			<i>CHARM-CKV</i>	0.912 $\pm$ 0.027	0.713 $\pm$ 0.030	0.842 $\pm$ 0.041	0.756 $\pm$ 0.043	0.591 $\pm$ 0.046
			<i>CHARM-CQ</i>	0.890 $\pm$ 0.021	<b>0.770 <math>\pm</math> 0.041</b>	<b>0.857 <math>\pm</math> 0.028</b>	<b>0.808 <math>\pm</math> 0.045</b>	<b>0.704 <math>\pm</math> 0.058</b>
CHB-MIT	17	2	Baseline	<b>0.658 <math>\pm</math> 0.009</b>	0.371 $\pm$ 0.014	0.296 $\pm$ 0.014	0.363 $\pm$ 0.012	0.439 $\pm$ 0.029
			<i>CHARM-base</i>	0.554 $\pm$ 0.006	0.504 $\pm$ 0.010	0.523 $\pm$ 0.012	0.503 $\pm$ 0.013	0.487 $\pm$ 0.016
			<i>CHARM-CKV</i>	0.562 $\pm$ 0.009	0.518 $\pm$ 0.011	0.543 $\pm$ 0.009	0.529 $\pm$ 0.007	0.504 $\pm$ 0.009
			<i>CHARM-CQ</i>	0.576 $\pm$ 0.009	<b>0.541 <math>\pm</math> 0.009</b>	<b>0.560 <math>\pm</math> 0.010</b>	<b>0.550 <math>\pm</math> 0.010</b>	<b>0.530 <math>\pm</math> 0.014</b>

**Table 2.** Performance when masking half of the brain, along a vertical or horizontal axis.

Augmentation	Method	Clean	Horizontal		Vertical	
			Group <sub>A</sub>	Group <sub>B</sub>	Group <sub>A</sub>	Group <sub>B</sub>
None	Baseline	<b>0.951 <math>\pm</math> 0.007</b>	0.631 $\pm$ 0.050	0.430 $\pm$ 0.043	0.486 $\pm$ 0.028	0.586 $\pm$ 0.052
	<i>CHARM-CKV</i>	0.900 $\pm$ 0.034	0.790 $\pm$ 0.032	0.600 $\pm$ 0.023	0.683 $\pm$ 0.033	0.762 $\pm$ 0.041
	<i>CHARM-CQ</i>	0.899 $\pm$ 0.018	<b>0.839 <math>\pm</math> 0.030</b>	<b>0.707 <math>\pm</math> 0.056</b>	<b>0.751 <math>\pm</math> 0.040</b>	<b>0.824 <math>\pm</math> 0.028</b>
CMSAugment	Baseline	<b>0.873 <math>\pm</math> 0.024</b>	0.823 $\pm$ 0.037	0.762 $\pm$ 0.02	0.779 $\pm$ 0.036	0.783 $\pm$ 0.03
	<i>CHARM-CKV</i>	0.829 $\pm$ 0.038	<b>0.850 <math>\pm</math> 0.029</b>	<b>0.778 <math>\pm</math> 0.034</b>	<b>0.794 <math>\pm</math> 0.037</b>	<b>0.853 <math>\pm</math> 0.022</b>
	<i>CHARM-CQ</i>	0.734 $\pm$ 0.224	0.750 $\pm$ 0.217	0.702 $\pm$ 0.200	0.711 $\pm$ 0.203	0.739 $\pm$ 0.213

**Table 3.** Out of domain transfer results on CHB-MIT with a model pre-trained on TUH Seizure dataset.

Method	Fixed	Fine-tuned
Baseline (in-domain)	0.891 $\pm$ 0.038	
Baseline (transfer)	0.757 $\pm$ 0.004	<b>0.963 <math>\pm</math> 0.015</b>
<i>CHARM-CKV</i>	<b>0.805 <math>\pm</math> 0.008</b>	0.942 $\pm$ 0.020
<i>CHARM-CQ</i>	0.795 $\pm$ 0.006	0.915 $\pm$ 0.026

Seizure, we pad them with zero channels. In Table 3, we report the results of the baseline CNN along with channel remapping modules, where the in-domain baseline is the model directly trained on the CHB-MIT dataset, i.e., no transfer is performed. We observe that the representations learned with *CHARM* transfer better than the baseline when freezing the transferred layers. This shows that our system allows for pre-training and transfer of embeddings across heterogeneous datasets. Interestingly, if we fine-tune the entire network, then the baseline (transfer) is able to relearn low-level representations and improves significantly over the in-domain baseline. To the best of our knowledge, this is the first time that a deep EEG classifier demonstrates out-of-domain transfer to a dataset recorded

with a different headset over different subjects.

#### 4. CONCLUSION

We introduce *CHARM*, a channel remapping model for training a single neural network across heterogeneous EEG data. Our model identifies the location of each channel from their content and remaps them to a canonical ordering by predicting a reordering matrix. This allows further processing by standard classifiers that expect a consistent channel ordering. Our differentiable reordering module leverages attention mechanisms and can be trained on data without information on the channel placement. We complement this model with a new data augmentation technique and demonstrate the efficiency of our approach over three EEG classification tasks, where various types of headsets can result in inconsistent channel orderings and numbers. In particular, we successfully transfer parameters across datasets with different collection protocols. This is an important result since available EEG data are currently fragmented across a wide variety of heterogeneous datasets. We believe that the robustness of our method will pave the way to training a single model across large-scale collections of heterogeneous data. Moreover, our approach is general enough to benefit other domains with varying sensor placements and numbers, including weather modeling, seismic activity monitoring and speech enhancement from microphone arrays.

## 5. REFERENCES

- [1] Robin Kennett, "Modern electroencephalography," *Journal of neurology*, vol. 259, no. 4, pp. 783–789, 2012.
- [2] Eva Svanborg and Christian Guilleminault, "EEG frequency changes during sleep apneas," *Sleep*, vol. 19, no. 3, pp. 248–254, 1996.
- [3] Henri Korkalainen, Juhani Aakko, Sami Nikkonen, Samu Kainulainen, Akseli Leino, Brett Duce, Isaac O Afara, Sami Myllymaa, Juha Töyräs, and Timo Leppänen, "Accurate deep learning-based sleep staging in a clinical population with suspected obstructive sleep apnea," *IEEE journal of biomedical and health informatics*, vol. 24, no. 7, pp. 2073–2081, 2019.
- [4] Akara Supratak, Hao Dong, Chao Wu, and Yike Guo, "Deep-sleepnet: A model for automatic sleep stage scoring based on raw single-channel eeg," *IEEE Transactions on Neural Systems and Rehabilitation Engineering*, vol. 25, no. 11, pp. 1998–2008, 2017.
- [5] Gert Pfurtscheller and Christa Neuper, "Motor imagery and direct brain-computer communication," *Proceedings of the IEEE*, vol. 89, no. 7, pp. 1123–1134, 2001.
- [6] NR Galloway, "Human brain electrophysiology: Evoked potentials and evoked magnetic fields in science and medicine," *The British journal of ophthalmology*, vol. 74, no. 4, pp. 255, 1990.
- [7] Feng Li, Guangfan Zhang, Wei Wang, Roger Xu, Tom Schnell, Jonathan Wen, Frederic McKenzie, and Jiang Li, "Deep models for engagement assessment with scarce label information," *IEEE Transactions on Human-Machine Systems*, vol. 47, no. 4, pp. 598–605, 2016.
- [8] Ali H Shoeb and John V Guttag, "Application of machine learning to epileptic seizure detection," in *Proceedings of the 27th International Conference on Machine Learning (ICML-10)*, 2010, pp. 975–982.
- [9] Alexander Craik, Yongtian He, and Jose L Contreras-Vidal, "Deep learning for electroencephalogram (eeg) classification tasks: a review," *Journal of neural engineering*, vol. 16, no. 3, 2019.
- [10] DF Wulsin, JR Gupta, Ram Mani, JA Blanco, and B Litt, "Modeling electroencephalography waveforms with semi-supervised deep belief nets: fast classification and anomaly measurement," *Journal of neural engineering*, vol. 8, no. 3, pp. 036015, 2011.
- [11] Yuanfang Ren and Yan Wu, "Convolutional deep belief networks for feature extraction of eeg signal," in *2014 International joint conference on neural networks (IJCNN)*. IEEE, 2014, pp. 2850–2853.
- [12] Yousef Rezaei Tabar and Ugur Halici, "A novel deep learning approach for classification of eeg motor imagery signals," *Journal of neural engineering*, vol. 14, no. 1, pp. 016003, 2016.
- [13] Robin Tibor Schirrmeyer, Jost Tobias Springenberg, Lukas Dominique Josef Fiederer, Martin Glasstetter, Katharina Eggensperger, Michael Tangermann, Frank Hutter, Wolfram Burgard, and Tonio Ball, "Deep learning with convolutional neural networks for eeg decoding and visualization," *Human brain mapping*, vol. 38, no. 11, pp. 5391–5420, 2017.
- [14] Vernon J Lawhern, Amelia J Solon, Nicholas R Waytowich, Stephen M Gordon, Chou P Hung, and Brent J Lance, "Eegnet: a compact convolutional neural network for eeg-based brain-computer interfaces," *Journal of neural engineering*, vol. 15, no. 5, pp. 056013, 2018.
- [15] Pierre Thodoroff, Joelle Pineau, and Andrew Lim, "Learning robust features using deep learning for automatic seizure detection," in *Machine learning for healthcare conference*, 2016, pp. 178–190.
- [16] Mengni Zhou, Cheng Tian, Rui Cao, Bin Wang, Yan Niu, Ting Hu, Hao Guo, and Jie Xiang, "Epileptic seizure detection based on eeg signals and cnn," *Frontiers in neuroinformatics*, vol. 12, pp. 95, 2018.
- [17] Shu Lih Oh, Yuki Hagiwara, U Raghavendra, Rajamanickam Yuvaraj, N Arunkumar, M Murugappan, and U Rajendra Acharya, "A deep learning approach for parkinson's disease diagnosis from eeg signals," *Neural Computing and Applications*, pp. 1–7, 2018.
- [18] Fatemeh Fahimi, Zhuo Zhang, Wooi Boon Goh, Tih-Shi Lee, Kai Keng Ang, and Cuntai Guan, "Inter-subject transfer learning with an end-to-end deep convolutional neural network for eeg-based bci," *Journal of neural engineering*, 2019.
- [19] Shivarudhrappa Raghu, Natarajan Sriraam, Yasin Temel, Shyam Vasudeva Rao, and Pieter L Kubben, "Eeg based multi-class seizure type classification using convolutional neural network and transfer learning," *Neural Networks*, 2020.
- [20] Dongrui Wu, Brent Lance, and Vernon Lawhern, "Transfer learning and active transfer learning for reducing calibration data in single-trial classification of visually-evoked potentials," in *2014 IEEE International Conference on Systems, Man, and Cybernetics (SMC)*. IEEE, 2014.
- [21] Dongrui Wu, Vernon J Lawhern, W David Hairston, and Brent J Lance, "Switching eeg headsets made easy: Reducing offline calibration effort using active weighted adaptation regularization," *IEEE Transactions on Neural Systems and Rehabilitation Engineering*, vol. 24, no. 11, pp. 1125–1137, 2016.
- [22] Ashish Vaswani, Noam Shazeer, Niki Parmar, Jakob Uszkoreit, Llion Jones, Aidan N Gomez, Łukasz Kaiser, and Illia Polosukhin, "Attention is all you need," in *Advances in neural information processing systems*, 2017.
- [23] Jimmy Lei Ba, Jamie Ryan Kiros, and Geoffrey E Hinton, "Layer normalization," *arXiv preprint arXiv:1607.06450*, 2016.
- [24] Kaiming He, Xiangyu Zhang, Shaoqing Ren, and Jian Sun, "Delving deep into rectifiers: Surpassing human-level performance on imagenet classification," in *Proceedings of the IEEE international conference on computer vision*, 2015, pp. 1026–1034.
- [25] Dmitry Ulyanov, Andrea Vedaldi, and Victor Lempitsky, "Instance normalization: The missing ingredient for fast stylization," *arXiv preprint arXiv:1607.08022*, 2016.
- [26] Diederik P Kingma and Jimmy Ba, "Adam: A method for stochastic optimization," *arXiv preprint arXiv:1412.6980*, 2014.
- [27] Iyad Obeid and Joseph Picone, "The temple university hospital eeg data corpus," *Frontiers in neuroscience*, vol. 10, 2016.
- [28] Ali Hossam Shoeb, *Application of machine learning to epileptic seizure onset detection and treatment*, Ph.D. thesis, Massachusetts Institute of Technology, 2009.